



Cite this: *RSC Appl. Interfaces*, 2024, 1, 430

Received 1st December 2023,  
Accepted 4th March 2024

DOI: 10.1039/d3lf00239j

[rsc.li/RSCApplInter](https://rsc.li/RSCApplInter)

## Prolonging the n-type conduction of thermoelectric carbon nanotubes exposed to warm air by mixing hydrated water into the adsorbed dopant layers composed of Li<sup>+</sup>-receptor molecules†

Shinichi Hata, <sup>\*a</sup> Chika Nakagawa, <sup>b</sup> Ayako Taketoshi, <sup>c</sup> Toru Murayama, <sup>ad</sup> Tamao Ishida, <sup>a</sup> Yukou Du, <sup>e</sup> Yukihide Shiraishi <sup>\*b</sup> and Naoki Toshima <sup>bf</sup>

**Mixing hydrated water into the dopant layer prolongs the operational stability of n-type carbon nanotubes (CNTs). Supramolecular interactions with Li<sup>+</sup> increase the water adsorption of the dopant layer, hinder atmospheric oxygen from entering the CNT structure, and extend the n-type lifetime at 373 K from 6 to 16 d.**

Semiconductor technology is advancing rapidly, creating a demand for low-cost, environmentally friendly, and sustainable technologies such as organic solar cells,<sup>1</sup> field-effect transistors,<sup>2</sup> and wearable devices.<sup>3</sup> Carbon nanotubes (CNTs) show promise for meeting these requirements.<sup>4–6</sup> Thus, the use of dopant molecules that electronically oxidize or reduce CNTs to control their p- or n-type semiconductor properties can effectively prevent irreversible CNT crystal damage, thereby preserving their quality and properties.<sup>7</sup> However, the electronic properties (thermoelectromotive force and local density of states) of CNTs with large specific surface areas (200–1000 m<sup>2</sup> g<sup>-1</sup>)<sup>8</sup> have not resolved the critical issue that n-type CNTs are easily p-doped, especially owing to the molecular adsorption of molecules, *e.g.*, oxygen from the

atmosphere, and its resulting electron acceptance.<sup>9,10</sup> In addition, polyethyleneimine, a pioneering electron-donating polymer, has been successfully and unsuccessfully used for long-term n-type conversion in the ambient environment.<sup>11–13</sup> The ambivalent levels of success can be attributed to concentration-controlled parameters such as dopant coverage, CNT's specific surface area, and chemical interactions between the dopant and CNT. The design of n-materials for future CNT-based thermoelectric (TE) devices that recover and utilize waste heat (<423 K) suggests that more rigorous fundamental studies on stabilizing n-type properties are needed to understand how heterogeneous material interfaces affect function.<sup>14</sup> To develop high-performance n-type CNTs with long-term reliability for TE devices, sequential doping of CNT surfaces with hydroxide or halide anions and stabilizing negative charges with ammonium or alkali metal cations appear promising.<sup>15</sup> For example, Na<sup>+</sup> or K<sup>+</sup> complexing crown ether cations<sup>16</sup> and positive charges in the bicyclic guanidine base-conjugated acid state<sup>17</sup> helped suppress atmospheric oxygen adsorption at high temperatures and extended the n-type conduction lifetime of CNTs in air (>30 d at 423 K<sup>16</sup>) and >6 months at 373 K.<sup>17</sup> Furthermore, in CNT samples with characteristically small specific surface areas (<100 m<sup>2</sup> g<sup>-1</sup>), an adsorbed molecular layer consisting of a phosphonium salt surfactant has been suggested to block water molecules and oxygen molecules (at 353 K) from directly contacting doping sites, stabilizing the delocalized negative charge of the CNT.<sup>18</sup> For high-temperature applications, investigating how the size, charge density, and hydrophilicity/hydrophobicity of the dopant shell covering the negatively charged doping sites affect the n-type conduction lifetime and developing facile techniques to improve the oxygen shielding function of the dopant shell and the oxygen permeability of the matrix would provide valuable insights.

In this study, as part of our investigation on the effectiveness of alkali metal ions, we focused on n-dopant

<sup>a</sup> Department of Applied Chemistry for Environment, Graduate School of Urban Environmental Sciences, Tokyo Metropolitan University, 1-1 Minami-Osawa, Hachioji, Tokyo 192-0397, Japan. E-mail: shinhta@tmu.ac.jp

<sup>b</sup> Department of Applied Chemistry, Faculty of Engineering, Sanyo-Onoda City University, Daigaku-Dori, 1-1-1, Sanyo-Onoda, Yamaguchi 756-0884, Japan. E-mail: shiraishi@rs.soci.ac.jp

<sup>c</sup> Department of Advanced Materials Chemistry, Graduate School of Engineering, Yokohama National University, 79-5 Tokiwadai, Hodogaya-ku, Yokohama 240-8501, Japan

<sup>d</sup> Yantai Key Laboratory of Gold Catalysis and Engineering, Shandong Applied Research Center of Gold Nanotechnology (AU-SDARC), School of Chemistry & Chemical Engineering, Yantai University, 30 Qingquan Road, Yantai 264005, China

<sup>e</sup> College of Chemistry, Chemical Engineering and Materials Science, Soochow University, Suzhou 215123, PR China

<sup>f</sup> Tokyo University of Science Yamaguchi, Japan

† Electronic supplementary information (ESI) available. See DOI: <https://doi.org/10.1039/d3lf00239j>



candidates, trinuclear metallomacrocycle compounds capable of recognizing and extracting  $\text{Li}^+$  in water that can assemble ruthenium complexes with tridentate ligands (Fig. 1).<sup>19</sup> In this receptor molecule, three oxygen-donating atoms are pre-organized for the complexation of  $\text{Li}^+$ , and the extreme polarity of the metal–oxygen bonds in the complex electrostatically favors the coordination of smaller  $\text{Li}^+$  over  $\text{Na}^+$ . This study provides preliminary insights into the preparation of n-type CNTs for warm air based on the properties of the adsorbed molecular layer on the CNT surface.

The ESI† provides details on the materials, experimental methods, and structural determination; the CNT films were prepared on a base polyimide sheet, and water, rather than organic solvents, was used as the dopant.<sup>20</sup> In addition, no encapsulation was used, thus enabling the study of the effects of  $\text{Li}^+$ . Fig. 2 shows the TE characteristics ( $S$  values,  $\sigma$  values, and output factor ( $\text{PF} = S^2\sigma$ ) values) of the fabricated films in the range of 330–390 K. The results show that regardless of the presence of  $\text{Li}^+$ , the  $S$  values of the CNTs are consistently negative, independent of temperature, with values ranging from  $-40.2$  to  $-46.0 \mu\text{V K}^{-1}$ . Considering that pure CNTs are p-type semiconductors ( $62.3 \mu\text{V K}^{-1}$ ), the receptor shows that without  $\text{Li}^+$ , dopants induce the conversion of holes to electrons over a broad temperature range. Importantly,  $\text{Li}^+$ -receptor/CNTs yield higher  $\sigma$  values ( $386\text{--}404 \text{ S cm}^{-1}$ ) than those yielded by receptor/CNTs. With increased  $\sigma$  values,  $\text{Li}^+$ -receptor/CNTs demonstrate a higher PF than receptor/CNTs, with a maximum of  $74.2 \mu\text{W m}^{-1} \text{ K}^{-2}$ , which is  $\sim 1.8$  times that of the receptor/CNT. Scanning electron microscopy (SEM) images of the macroscopic CNT structure within the film (which contributes to the electrical conductivity – see Fig. S1†) reveal that adding  $\text{Li}^+$  decreases the CNT bundle diameter from  $52.1 \pm 20.8 \text{ nm}$  to  $27.1 \pm 11.8 \text{ nm}$ , making it very fine. Scanning transmission electron microscopy-energy dispersive X-ray spectroscopy (STEM-EDX, Fig. S2 and S3†) confirmed that the dopants used as dispersants were wrapped around the fibrous CNTs.

The CNT structure within the composite film and the degree of dopant/CNT interactions were confirmed by Raman spectroscopy. Focusing on the extended region of the radial breathing mode (RBM) band indicates that the addition of the receptor or  $\text{Li}^+$ -receptor to the composite film reduces the intensity of the original CNT peak (Fig. S4(a)†), thus

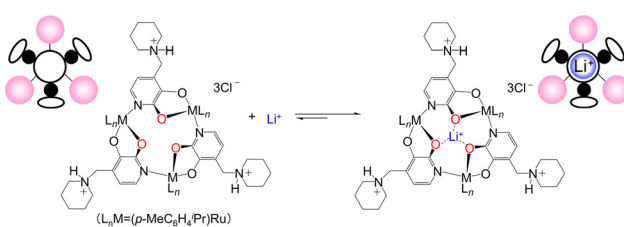


**Fig. 1** Structure of a trinuclear metallomacrocycle compound (receptor) designed for selective complexation with  $\text{Li}^+$  in water. The three pre-organized oxygen-donating atoms facilitate complexation with  $\text{Li}^+$ , and the high metal–oxygen bond polarity in the complex effectively entraps  $\text{Li}^+$  due to electrostatic reasons.

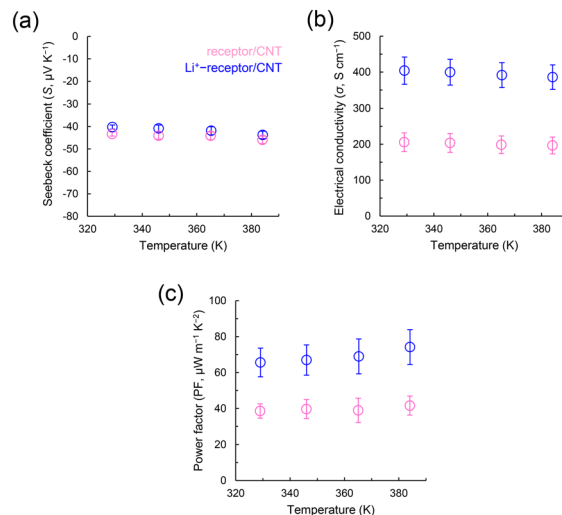


**Fig. 2** (a) Seebeck coefficient, (b) electrical conductivity, and (c) power factor of the receptor/carbon nanotube (CNT) (pink) and  $\text{Li}^+$ -receptor/CNT (blue) plotted against temperature.

indicating that (in both cases) the adsorbed dopant on the CNT wall interferes with the expansion/contraction oscillations of the CNTs.<sup>21</sup> Fig. S4(b)† shows the normalized spectra of the G band associated with carbon atom vibrations along the CNT plane; the G band is located at  $1589$ ,  $1590$ , and  $1592 \text{ cm}^{-1}$  in the original state, receptor, and  $\text{Li}^+$ -receptor/CNT cases, respectively.<sup>22</sup> The larger blue shift with  $\text{Li}^+$  indicates stronger electrostatic interactions between the dopant and CNTs. Additionally, the observed D/G ratio values ( $0.019 \pm 0.004$ ) are very similar among the samples, and the CNT walls showed no significant defects or new functional groups after doping.

In addition,  $\text{N}_2$  (at  $77 \text{ K}$ ) and  $\text{H}_2\text{O}$  (at  $298 \text{ K}$ ) adsorption isotherms were recorded to investigate the accessibility of negatively charged doping sites to oxygen within the CNTs and the water adsorption capacity of the dopant layer;  $\text{N}_2$  is highly adsorbed on the CNTs, whereas it is barely adsorbed onto the doped samples (Fig. 3(a)). This implies that the dopant molecules coating the CNT surface cause a substantial decrease in the bare CNT area available for  $\text{N}_2$  adsorption. Conversely, water is adsorbed minimally on the

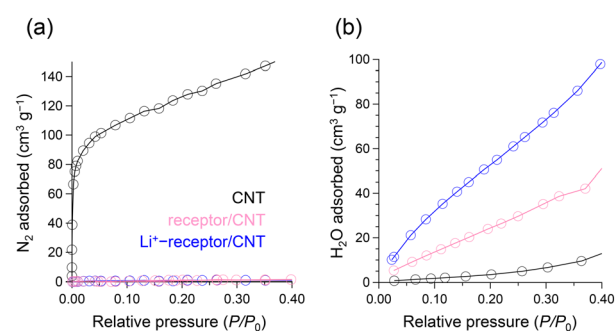


**Fig. 3** (a)  $\text{N}_2$  adsorption isotherms at  $77 \text{ K}$ . (b) Water-vapor adsorption isotherms at  $298 \text{ K}$ .



CNT samples because graphene structures are inherently hydrophobic, whereas water is specifically adsorbed on both doped samples (Fig. 3(b)). Interestingly, the volumes of the adsorbed  $\text{H}_2\text{O}$  monolayers were 38.3 and 68.9  $\text{cm}^3 \text{ g}^{-1}$  for receptor/CNT and  $\text{Li}^+$ -receptor/CNT, respectively, indicating increases following the inclusion of  $\text{Li}^+$ . This provides important evidence that increasing the ionic nature of the dopant shell on the CNT surface increases the water adsorption capacity of the adsorbed molecular layer.

Both samples were aged in the dark, air, and in a blow box at 373 K to evaluate their n-type lifetimes, and the TE properties were monitored periodically (Fig. 4). However, the n-lifetimes were at least 6 and 16 d for the receptor/CNT and  $\text{Li}^+$ -receptor/CNT, respectively, thus indicating the stabilization effect of  $\text{Li}^+$ . The minimum  $\sigma$  value is also consistent with a crossover from negative to positive  $S$  values, as expected in a sample where the p-dopant oxygen molecules and n-dopants mutually compensate for each other.<sup>23</sup> The results provide interesting insights into n-type stabilization under thermal oxygen conditions, thus suggesting that, unlike bare receptors, the adsorbed dopant layer in  $\text{Li}^+$ -receptors suppresses electrophilic reactions with molecular oxygen, thus hindering p-type doping.

Although we used water to disperse the CNTs during film conditioning work, electrons can be donated from  $\text{Cl}^-$  to CNTs in water based on the redox potential.<sup>24</sup> The  $\text{Cl}^-$  in the receptor molecules (used as dispersants and dopants) appears to have induced n-type properties by generating some negatively charged sites on the CNT walls, thus increasing the Fermi energy of the CNTs relative to their initial energy state.<sup>25</sup> Furthermore, the delocalized negative charge on the CNT surface satisfies the charge neutrality rule with the cationic receptor directly adsorbing molecules on the CNT wall. In other words, the receptor acts as a counterion for n-type CNTs based on strong molecular adsorption and ionic interactions at the CNT surface. The  $S$  values of the receptor/CNTs did not significantly change with  $\text{Li}^+$  loading, and the CNT Fermi level did not shift. This suggests that as the receptor is a molecule with bulky substituent arms with trinuclear geometry, the three ammonium salts at its molecular ends may be directly

responsible for the energy levels of the CNTs. Fortunately, however, the results show that adding  $\text{Li}^+$  benefited the  $\sigma$  values. During CNT dispersion, their surfaces become more hydrophilic owing to the adsorption of the receptor molecules. This weakens the strong hydrophobic interactions between CNTs and the strong van der Waals attraction between graphene structures, thus allowing the CNT bundles to detach.<sup>26</sup> In contrast, loading the receptor with  $\text{Li}^+$  increases both the ionicity within the adsorbed molecules and the hydrophilicity of the CNT surface, further dispersing the CNTs. This finding is also supported by actual SEM and STEM-EDX observations. In other words, the narrower CNT bundles create an interconnected network structure that increases the number of conduction pathways available for charge transport, which would crucially contribute to the enhancement of  $\sigma$ .<sup>27,28</sup> Consequently, the PF value of n-type TE films increased 1.8-fold when the receptor molecules were loaded with  $\text{Li}^+$ .

Essentially, the outermost surface of the CNT experiences molecular oxygen oxidation, which directly affects the n-doping lifetime. Thus, negatively charged surfaces are more susceptible to attacks by molecular oxygen. In contrast,  $\text{Li}^+$ -receptor/CNTs, which form narrower bundles than receptor/CNTs, have an n-state that lasts up to 10 d at elevated temperatures, thus indicating the presence of an n-stabilizing factor at the material surface. The decreased intensity in the RBM suggests noncovalent adsorption of receptor molecules on the outer CNT wall irrespective of whether  $\text{Li}^+$  is present (Fig. S4(a)†).<sup>26</sup> However, adding  $\text{Li}^+$  leads to a considerable shift in the G band (Fig. S4(b)†). This behavior is commonly observed in CNTs wrapped with cationic amphiphiles and polymers and is predicted to depend on the cationic charge coverage.<sup>22,29</sup> In other words, this behavior suggests that  $\text{Li}^+$ -receptor molecules contribute more to the charge density of the layer of adsorbed molecules (coating the CNTs) than the contributions of receptor molecules. The  $\text{H}_2\text{O}$  adsorption isothermal measurements revealed that  $\text{Li}^+$  loading enhanced the hydrophilicity of the receptor molecule film on the CNT surface (Fig. 3(b)). Thermogravimetric measurements of both samples showed that  $\text{Li}^+$  loading increased the amount of hydrated water (Fig. S5†).<sup>30,31</sup> The apparent weight loss of adsorbed water in the range of 323–443 K was 6.1%, which corresponds to 17 water molecules per  $\text{Li}^+$ -receptor molecule. The increased hydrophilicity of the chemical structure of the  $\text{Li}^+$ -receptor allows it to bind chemically to water vapor molecules through noncovalent interactions (e.g., hydrogen bonding or electrostatic), thus resulting in an increased retention of water molecules within the dopant layer.<sup>32</sup> The factor responsible for the improved n-stability in the 373 K atmosphere is the slower diffusion penetration of thermally active oxygen molecules into the CNT structure relative to those into the cationic dopant layer; this is owing to the physical exclusion of water molecules chemically supplemented by  $\text{Li}^+$  on the adsorbed receptor layer on the CNT surface (Fig. 5). This kinetically suppresses the electrophilic oxidation reactions that occur between the

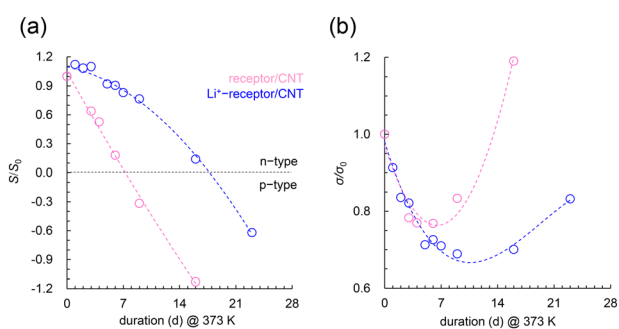
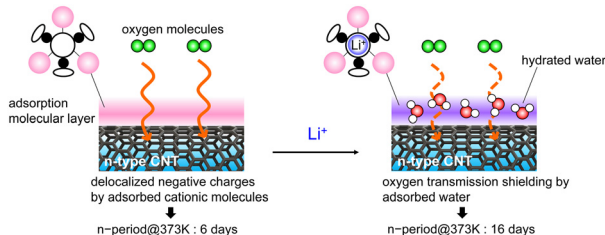


Fig. 4 Stability of unencapsulated receptor/CNT and  $\text{Li}^+$ -receptor/CNT in air at 373 K. (a) n-type seebeck coefficient to the initial n-type seebeck coefficient ( $S/S_0$ ), and (b) electrical conductivity to the initial electrical conductivity ( $\sigma/\sigma_0$ ) over duration.





**Fig. 5** Adsorption layers of receptor molecules (left) and  $\text{Li}^+$ -receptor molecules (right) on a CNT. In the adsorbed layer of  $\text{Li}^+$ -receptor, chemisorbed water molecules impede the ingress and diffusion of atmospheric oxygen, thereby postponing its access to electronically active sites on the CNT.

electron-active sites of the CNTs and oxygen. Recently, CNTs wrapped in cationic surfactants retained their n-doped state for more than 28 d after water exposure. Preliminary findings also indicated that the hydrophilic dopant layer's hydratable shell structure prevents contact between the CNT surface and impurities.<sup>20,33</sup> Although advanced characterizations are still needed, this study reveals that hydrated water molecules can suppress the p-doping caused by oxygen present in the thermal ambient of the dopant layer. This is a previously uncharacterized effect of dopants on the stability of n-type materials in high-temperature applications and provides important fundamental insights toward promising material design strategies.

In summary, this study provides new evidence that the receptor's ability to load  $\text{Li}^+$  can be exploited to increase the dopant layer hydrophilicity on the CNT surface, thus resulting in moderate dispersion of the CNT bundle and increases in the  $\sigma$  value and n-type thermal TE output of the CNTs. Furthermore, the increased charge density due to  $\text{Li}^+$  in the adsorption film covering the negatively charged doping sites of the CNTs increases the water adsorption capacity. As a result, the n-type lifetime of CNTs is extended from 6 to 16 d because oxygen molecules are physically prevented from permeating the dopant layer under high-temperature air conditions, thus hindering p-type doping. To comprehensively understand supramolecular/CNT nanocomposites, their detailed electronic structures and carrier transport properties should be studied as a basis for future research on TE materials. Studies of n-type conduction lifetimes under systematically controlled relative air-humidity conditions are an important future work in advancing complex n-type materials research. Specifically, these studies must unravel the physical and chemical mechanisms based on which oxygen is associated with reduced stability and must perform detailed quantitative comparisons of time constants for water evaporation (or evaporation rate) and dedoping. This important study will drive the development of complex n-type materials research in the future. Hydratable hydrophilic dopant/nanotube interface engineering used to design dopant shells for warm air is key to solving the chemical instability problem of n-type materials and can serve as an important technology for the development of film-based TE generators for high-temperature applications.

## Author contributions

S. H. and Y. S. conceived the original concept and designed the experiments. S. H. wrote the manuscript. S. H. and C. N. synthesized and characterized the materials. A. T. conducted the thermogravimetry and analysis. T. M. measured and analyzed the  $\text{N}_2$  and  $\text{H}_2\text{O}$  adsorption. T. I. performed the STEM-EDX measurements. Y. D. and N. T. provided advice for interpreting the results. S. H. and Y. S. supervised the project. All authors contributed to the discussion of the results.

## Conflicts of interest

There are no conflicts to declare.

## Acknowledgements

This study was supported in part by KAKENHI projects (No. 21K14428 to S. H., 23H01763 to T. M., and 23K04399 to Y. S.) from the JSPS, Tanigawa Thermal Technology Promotion Fund, and the Environmental research grant from Steel Foundation for Environmental Protection Technology, Japan.

## Notes and references

- 1 Z. Li, V. Saini, E. Dervishi, V. P. Kunets, J. Zhang, Y. Xu, A. R. Biris, G. J. Salamo and A. S. Biris, *Appl. Phys. Lett.*, 2010, **96**, 033110.
- 2 A. Javey, R. Tu, D. B. Farmer, J. Guo, R. G. Gordon and H. Dai, *Nano Lett.*, 2005, **5**, 345.
- 3 S. Patel, H. Park, P. Bonato, L. Chan and M. Rodgers, *J. Neuroeng. Rehabil.*, 2012, **9**, 21.
- 4 C. Yu, Y. S. Kim, D. Kim and J. C. Grunlan, *Nano Lett.*, 2008, **8**, 4428.
- 5 N. Toshima, *Synth. Met.*, 2017, **225**, 3.
- 6 Y. Zhang, Q. Zhang and G. Chen, *Carbon Energy*, 2020, **2**, 408.
- 7 T. Fujigaya and N. Nakashima, *Sci. Technol. Adv. Mater.*, 2015, **16**, 024802.
- 8 K. Kobashi, S. Ata, T. Yamada, D. N. Futaba, T. Okazaki and K. Hata, *ACS Appl. Nano Mater.*, 2019, **2**, 4043.
- 9 J. Kong, N. R. Franklin, C. Zhou, M. G. Chapline, S. Peng, K. Cho and H. Dai, *Science*, 2000, **287**, 622.
- 10 P. G. Collins, K. Bradley, M. Ishigami and A. Zettl, *Science*, 2000, **287**, 1801.
- 11 D. D. Freeman, K. Choi and C. Yu, *PLoS One*, 2012, **7**, e47822.
- 12 C. Yu, A. Murali, K. Choi and Y. Ryu, *Energy Environ. Sci.*, 2012, **5**, 9481.
- 13 W. Zhou, Q. Fan, Q. Zhang, L. Cai, K. Li, X. Gu, F. Yang, N. Zhang, Y. Wang, H. Liu, W. Zhou and S. Xie, *Nat. Commun.*, 2017, **8**, 14886.
- 14 J. L. Blackburn, A. J. Ferguson, C. Cho and J. C. Grunlan, *Adv. Mater.*, 2018, **30**, 1704386.
- 15 Y. Nonoguchi, *Carbon Rep.*, 2023, **2**, 146.
- 16 Y. Nonoguchi, M. Nakano, T. Murayama, H. Hagino, S. Hama, K. Miyazaki, R. Matsubara, M. Nakamura and T. Kawai, *Adv. Funct. Mater.*, 2016, **26**, 3021.



17 S. Horike, Q. Wei, K. Akaike, K. Kiriha, M. Mukaida, Y. Koshiba and K. Ishida, *Nat. Commun.*, 2022, **13**, 3517.

18 S. Hata, F. Kitano, H. Ihara, T. Murayama, Y. Du, Y. Shiraishi and N. Toshima, *ACS Appl. Eng. Mater.*, 2023, **1**, 894.

19 Z. Grote, M.-L. Lehaire, R. Scopelliti and K. Severin, *J. Am. Chem. Soc.*, 2003, **125**, 13638.

20 S. Hata, M. Shiraishi, S. Yasuda, G. Juhasz, Y. Du, Y. Shiraishi and N. Toshima, *Energy Mater. Adv.*, 2022, 9854657.

21 M. Baibarac, I. Baltog, C. Godon, S. Lefrant and O. Chauvet, *Carbon*, 2004, **42**, 3143.

22 V. A. Sinani, M. K. Gheith, A. A. Yaroslavov, A. A. Rakhnyanskaya, K. Sun, A. A. Mamedov, J. P. Wicksted and N. A. Kotov, *J. Am. Chem. Soc.*, 2005, **127**, 3463.

23 F. Abdallah, L. Ciammaruchi, A. Jiménez-Arguijo, E.-S. M. Duraia, H. S. Ragab, B. Dörling and M. Campoy-Quiles, *Adv. Mater. Technol.*, 2020, **5**, 2000256.

24 S. Horike, Q. Wei, K. Kiriha and M. Mukaida, *Chem. Phys. Lett.*, 2020, **755**, 137801.

25 Y. Nakashima, R. Yamaguchi, F. Toshimitsu, M. Matsumoto, A. Borah, A. Staykov, M. S. Islam, S. Hayami and T. Fujigaya, *ACS Appl. Nano Mater.*, 2019, **2**, 4703.

26 M. Wong, M. Paramsothy, X. J. Xu, Y. Ren, S. Li and K. Liao, *Polymer*, 2003, **44**, 7757.

27 F. Mirri, A. W. Ma, T. T. Hsu, N. Behabtu, S. L. Eichmann, C. C. Young, D. E. Tsentalovich and M. Pasquali, *ACS Nano*, 2012, **6**, 9737.

28 J. Jung, E. H. Suh, Y. J. Jeong, H. S. Yang, T. Lee and J. Jang, *ACS Appl. Mater. Interfaces*, 2019, **11**, 47330.

29 V. T. Tiong, N. D. Pham, T. Wang, T. Zhu, X. Zhao, Y. Zhang, Q. Shen, J. Bell, L. Hu and S. Dai, *Adv. Funct. Mater.*, 2018, **28**, 1705545.

30 C. G. Tang, M. N. Syafiqah, Q.-M. Koh, M. C.-Y. Ang, K.-K. Choo, M.-M. Sun, M. Callsen, Y.-P. Feng, L.-L. Chua, R.-Q. Png and P. K. H. Ho, *Nat. Commun.*, 2023, **14**, 3978.

31 S. Wang, X. Xu, C. Cui, C. Zeng, J. Liang, J. Fu, R. Zhang, T. Zhai and H. Li, *Adv. Funct. Mater.*, 2022, **32**, 2108805.

32 F. Deng, Z. Chen, C. Wang, C. Xiang, P. Poredoš and R. Wang, *Adv. Sci.*, 2022, **9**, 2204724.

33 S. Hata, K. Maeshiro, M. Shiraishi, S. Yasuda, Y. Shiozaki, K. Kametani, Y. Du, Y. Shiraishi and N. Toshima, *Carbon Energy*, 2023, **5**, e285.

